Supporting Information

de Peppo et al. 10.1073/pnas.1301190110

SI Methods

Materials. Dulbecco's modified eagle medium (DMEM), KnockOut DMEM (KO-DMEM), KnockOut Serum Replacement (KO-SR), Dulbecco's phosphate buffered saline solution (DPBS), GlutaMAX solution (100×), nonessential amino acids (100×), β-mercaptoethanol, penicillin-streptomycin solution (100×), trypsin/ethylenediaminetetraacetic acid (EDTA; 0.25%), bovine serum albumin fraction V (BSA), insulin, Na pyruvate (100×), insulin-transferrin-selenium supplement (ITS: 100×), TGF-β3, Geltrex, StemPro hESC serum- and feeder-free medium, DAPI, basic fibroblast growth factor (bFGF), and Alexa Fluor secondary antibodies were purchased from Life Technologies. HyClone fetal bovine serum (FBS), Tris buffer, proteinase K, PBS, and CitriSolv were purchased from Fisher Scientific. All other chemicals were purchased from Sigma-Aldrich unless otherwise noted.

Culture and Characterization of Pluripotent Stem Cell Lines. The hESC lines H9 and H13 were obtained from the WiCell Research Institute (www.wicell.org) and expanded on mouse embryonic fibroblasts (MEFs; GlobalStem) in medium consisting of KO-DMEM supplemented with 20% (vol/vol) KO-SR, 10 ng/mL bFGF, 2 mM GlutaMAX, 0.1 mM nonessential amino acids, 0.1 mM β-mercaptoethanol, and 100 U/mL penicillin-streptomycin. The hiPSC lines 11c and 1013A were generated from dermal fibroblasts obtained from healthy individuals using the retroviral vectors (11c) (1) and Sendai virus (1013A) (2) according to the previously published protocols and cultured on MEFs as described above for the line H9. The hiPSC line BC1 generated previously from bone marrow stromal cells using an episomal vector (3) was expanded on Geltrex in StemPro hESC serum- and feeder-free medium. Detailed information about the cell lines is presented in Fig. S1.

Before mesenchymal differentiation, expanded hiPSC lines were evaluated for the expression of pluripotency makers and karyotyped using standard G-banding (Cell Line Genetics). To investigate the expression of pluripotency markers, cultures were fixed in paraformaldehyde [4% (vol/vol); Polyscientific], permeabilized using 0.1% Triton X-100 in DPBS, blocked with 5% (vol/vol) donkey serum (Jackson ImmunoResearch Laboratories Inc.) in DPBS and incubated overnight with primary antibodies against TRA-1-60 (5 μg/mL; Millipore; MAB4360), Oct-4 (2.5 μg/mL; R&D Systems; AF1759), and Sox2 (2.5 μg/mL; Stemgent; 09-0024). Alexa Fluor secondary antibodies were used for detection (2 μg/mL; catalog nos. A31571, A11057, and A21206), and the nuclei were counterstained with DAPI (1 μg/mL). Fluorescence images were taken with an Olympus IX71 mounted with Q-Color 3 imaging camera and using the Olympus DP-BSW software, and processed with ImageJ. All fluorescent images are pseudocolors.

Cultures were regularly screened for mycoplasma using the MycoAlert Mycoplasma Detection Kit (Lonza). Briefly, culture media were centrifuged at 450 × *g* for 5 min, the supernatants collected, and luminescence measured using the Synergy Mx microplate reader and Gen5 software (BioTek).

Differentiation and Characterization of Mesenchymal Progenitors from hiPSCs and hESCs. Confluent cultures of H9 and hiPSC lines were treated with induction medium consisting of KO-DMEM supplemented with 20% (vol/vol) HyClone FBS, 2 mM GlutaMAX, 0.1 mM nonessential amino acids, 0.1 mM β-mercaptoethanol, and 100 U/mL penicillin-streptomycin as reported previously (4). After 1 wk, cells were detached using trypsin/EDTA and passaged at high density (10^5 cells per square centimeter; passage 1) to tissue culture flasks coated with gelatin (0.1%; EmbryoMax; Millipore). Upon reaching confluence, cells were passaged at regular density (10^4 cells per square centimeter) using trypsin/EDTA until they became homogenous for a fibroblastic-like morphology (passages 3–5). Cells were expanded under similar conditions up to passage 10 to investigate their proliferation potential. To assess the genomic stability of mesenchymal progenitors following in vitro expansion, karyotype analysis was performed at passage 10 for all lines investigated (Cell Line Genetics).

Surface antigen profile of hESC- and hiPSC-derived progenitors was evaluated at passage 5 using a panel of primary antibodies (BD Biosciences): Tra1-60 PE (catalog no. 560193), SSEA4 V450 (561156), SSEA1 PE (560142), CD14 PE (561707), CD31 PE (555446), CD34 PE (555822), CD45 PE (560975), HLA-A2 PE (558570), HLA-DM PE (555983), HLA-DR PE (556644), HLA-ABC PE (557349), B2M PE (551337), CD13 PE (555394), CD29 PE (555443), CD44 PE (561858), CD49e PE (555617), CD73 FITC (561254), CD81 PE (555676), CD90 PE (555596), CD151 PE (556057), AlkPhos (ALP) AF 647 (561500), CD49a PE (559596), CD49b PE (555669), CD49c PE (556025), CD49d PE (555503), CD49f PE (555736), CD51/61 PE (550037), CD54 PE (555511), CD140b PE (558821), CD146 PE (550315), CD56 PE (555516), CD63 PE (561925), CD102 PE (558080), CD104 PE (555720), CD106 PE (555647), CD166 PE (559263), CD184 PE (555974), CD271 PE (557196), mouse IgG1, kappa PE (555749), mouse IgM, kappa PE (559926), rat IgG2a, kappa PE (555844), rat IgG2b, kappa PE (555848), mouse IgG2a PE (555574), and CD133 APC (Miltenyi Biotec; 130-080-801).

For comparison, BMSC batches from our previous study were evaluated at passage 5 (9). Cells were enzymatically detached with trypsin/EDTA and filtered through a 70-μm cell strainer (BD Biosciences) to obtain a single-cell suspension. The 5×10^6 cells were resuspended in 3 mL of a sterile staining buffer [DPBS containing 0.5% (vol/vol) BSA, 100 U/mL penicillin/streptomycin, 2 mM EDTA, and 20 mM glucose]. The 50-μL aliquots of diluted primary antibodies were dispensed into black 96-well plates (Corning), followed by the addition of 50-μL aliquots containing 8×10^5 cells for a total of 100 μL per well. Cells were incubated on ice for 30 min in the dark, followed by washing with staining buffer, and analyzed immediately on BD Biosciences ARIA-IIu SOU Cell Sorter configured with a 100-μm ceramic nozzle and operating at 20-psi sheath fluid pressure. Data were acquired and analyzed using the Diva 6.0 software (BD Biosciences). Positive expression of surface markers was determined using a combination of fluorescent minus one and isotope controls. Gates were set using 1% in negative controls. Additional analysis of subpopulations coexpressing specific markers was done according to the gating hierarchy shown in Fig. S3*A*.

Differentiation potential of hESC- and hiPSC-derived progenitors was evaluated in monolayer and micromass pellet cultures. For monolayer cultures, cells at passage 5 were plated at 10^4 cells per square centimeter into gelatin-coated 24-well cell culture plates and cultured for 4 wk in (*i*) control medium [DMEM supplemented with 10% (vol/vol) HyClone FBS and 100 U/mL penicillin-streptomycin], (*ii*) osteogenic medium (control medium supplemented with 1 μM dexamethasone, 10 mM β-glycerophosphate, and 50 μM ascorbic acid-2-phosphate), and (*iii*) adipogenic induction medium (control medium supplemented with 1 μM dexamethasone, 10 μg/mL insulin, 200 μM indomethacin, and 500 μM 3-isobutyl-1-methylxanthine) 1 wk after reaching confluence, and adipogenic maintenance medium (control medium supplemented with 10 μg/mL insulin) until the end of the experimental period. At 2 and 4 wk after seeding, samples were har-

vested to investigate cell differentiation. Osteogenesis was evaluated by histological staining of alkaline phosphatase (ALP) activity using the Fast Blue RR Salt staining (Sigma-Aldrich), and von Kossa staining of calcium deposition following standard procedures. The amount of deposited calcium was determined biochemically using the Calcium LiquiColor Kit (Stanbio Laboratory) according to the manufacturer's protocol. Adipogenesis was assessed by Oil Red O staining of accumulated lipids following standard procedures. Images were quantified using ImageJ software. Positively stained areas were selected by hand and the area measured. The area stained positively was normalized to the total area, and expressed as percent of positive area. All images were taken at the same exposure settings.

For micromass pellet cultures, 3×10^5 cells at passage 5 were centrifuged at $300 \times g$ for 5 min, and cultured 4 wk in control medium (as above) and chondrogenic medium consisting of DMEM supplemented with 10% (vol/vol) HyClone FBS, 100 nM dexamethasone, 50 μg/mL ascorbic acid-2-phosphate, 40 μg/mL L-proline, 1% (vol/vol) ITS, 1 mM sodium pyruvate, 10 ng/mL TGF-β3, and 100 U/mL penicillin-streptomycin. For histological evaluations, pellets were fixed in 10% (vol/vol) formalin in DPBS for 24 h at room temperature, mounted in HistoGel (Fisher Scientific), embedded in paraffin, and sectioned at 5 μm. The presence of glycosaminoglycans (GAG) was evaluated by Alcian blue stain using standard procedures. The amount of deposited glycosaminoglycans was evaluated using the Blyscan sulfated GAG assay kit (Biocolor) according to the manufacturer's protocol. Before analysis, pellets were digested in 150 μL of digestion buffer [10 mM Tris, 1 mM EDTA, and 0.1% (vol/vol) Triton X-100] containing 0.1 mg/mL proteinase K overnight at 60 °C and homogenized using a powered pellet pestle (Sigma-Aldrich).

Decellularized Bone Scaffolds. Bone disks were prepared as previously described (4). Plugs of trabecular bone (4 mm diameter × 4 mm height) were drilled from the subchondral region of metacarpal joints of 2-wk to 4-mo-old calves (Green Village Packing). Soon after, plugs were cleansed under high-pressure streamed water to remove the bone marrow, and then sequentially washed with a solution of EDTA (0.1%) in PBS, EDTA (0.1%) in Tris (10 mM), and SDS (0.5%) in Tris (10 mM), followed by treatment with a solution of DNase and RNase in Tris buffer (10 mM) to remove cellular material. Decellularized bone plugs were thoroughly rinsed in PBS, freeze-dried, and cut to 4 mm in length. Each individual scaffold was weighted and measured to calculate the density, and those in the range of 0.37–0.45 mg/mm^3 were selected, sterilized in ethanol (70% vol/vol), and conditioned in osteogenic medium overnight before cell seeding.

Construct Assembly and Culture in Perfusion Bioreactors. Mesenchymal progenitors at passage 5 were suspended in osteogenic medium at a density of 30×10^6 cells/mL, and a 40-μL aliquot of the cell suspension was pipetted into the blot-dried scaffolds. Every 15 min, for 1 h, the scaffolds were flipped to facilitate uniform cell distribution; each time, 5 μL of medium was added to prevent the cells from drying out. Cell/scaffold constructs were then placed in six-well plates and incubated in osteogenic medium. After 3 d, constructs were transferred to each of the perfusion bioreactors and cultured in osteogenic medium for up to 5 wk. Two cell/scaffold constructs per line were kept under static conditions in six-well plates for the entire experimental period. Each bioreactor enabled uniform perfusion of six constructs, according to our established protocol (4). We selected a uniform flow rate of 3.6 mL/min corresponding to the interstitial velocity of 0.8 mm/s, which was set using a digital, low-flow, multichannel Masterflex peristaltic pump (Cole Palmer). These conditions were shown optimal in our previous work (4). Culture medium in the bioreactor was recirculated and maintained in equilibrium with the atmosphere in the incubator. Along the experimental period, 50% of the medium volume was exchanged twice a week with fresh medium, and aliquots collected for biochemical assays. Cell/scaffold constructs were harvested after 3 and 5 wk of culture, cut in half, weighed, and processed for biochemical and histological analyses.

Cell Survival and Proliferation in Engineered Bone Constructs. Constructs were harvested before transfer to bioreactors and after 3 and 5 wk of perfusion culture to assess survival and proliferation. Cells survival was investigated qualitatively using the LIVE/DEAD assay (Molecular Probes/Life Technologies) according to the manufacturer's protocol. Construct halves were washed in DPBS and incubated with a solution of calcein AM (2 μM) and ethidium bromide (4 μM) in RPMI medium without red phenol for 45 min and imaged by epifluorescence and confocal microscopy. Fluorescence images were taken with an Olympus IX71 as described above, and processed with ImageJ. Confocal images were takes with a Zeiss microscope (Axiovert 200M) mounted with LSM 5 Pascal exciter using the LSM 5 Pascal software under defined settings. All fluorescent images are pseudocolors.

The initial cell density before transfer to bioreactor, as well as cell proliferation after 3 and 5 wk under perfusion culture, were estimated by evaluating the DNA content using the Quant-iT PicoGreen dsDNA Assay Kit (Life Technologies) according to the manufacturer's protocol. Briefly, samples were digested in 1 mL of digestion buffer [10 mM Tris, 1 mM EDTA, and 0.1% (vol/vol) Triton X-100] containing 0.1 mg/mL proteinase K overnight at 60 °C. Samples were repeatedly vortexed to facilitate digestion. Supernatants were collected and diluted as necessary to work in the linear range of the assays. A standard curve of known concentrations of λ DNA was used to convert fluorescence to total DNA content.

All cultures were regularly screened for mycoplasma using the MycoAlert Mycoplasma Detection Kit as described previously.

ELISA. Medium samples were collected from bioreactors and static cultures at each medium change during the 5 wk of culture. Osteopontin release was assessed using the Quantikine ELISA Kit (R&D Systems) according to the manufacturer's instructions. Samples were centrifuged at $450 \times g$ for 5 min, and 50 μL of supernatant used for the analysis. Optical density was measured at 450 nm using the Synergy Mx microplate reader and Gen5 software (BioTek Instruments). Results were corrected by subtracting readings at 540 nm.

RNA Extraction and Real-Time PCR. Cells in monolayer were lysed in RLT buffer (Qiagen) and total RNA was extracted using the RNeasy Mini Kit (Qiagen) according to manufacturer's instructions. Cell/scaffold constructs were disintegrated in 1 mL of TRIzol (Ambion/Life Technologies) using steel balls and the Mini-Beadbeater (BioSpec). Suspensions were centrifuged at $12{,}000 \times g$ for 10 min at 4 °C to remove tissue debris and extracted with chloroform. The aqueous phase was collected, mixed with equal volume of 70% (vol/vol) ethanol, and RNA extracted using the RNeasy Mini Kit (Qiagen) as above. Purified RNA was reversely transcribed with random hexamers using the SuperScript III First-Strand Synthesis System (Life Technologies) in the Eppendorf Mastercycler Gradient. Real-time PCR was performed using the Stratagene Mx 3000P cycler (Agilent Technologies) in a 20-μL volume reaction using the TaqMan Universal PCR Master Mix and TaqMan Gene Expression Assays (Applied Biosystems/Life Technologies) composed of FAM dye-labeled TaqMan MGB probe and PCR primers for alkaline phosphatase (*ALP*; Hs01029144_m1), osteopontin (*OPN*; Hs00959010_m1), platelet-derived growth factor receptor beta (*PDGFRB*; Hs01019589_m1), and VIC dye-labeled TaqMan MGB probe and primers for the housekeeping gene glyceraldehyde 3-phosphate dehydrogenase (*GAPDH*, Hs02758991_g1). Cycling conditions were 95 °C for 10 min followed by 40 cycles of 95 °C for 15 s (denaturation) and 60 °C for 60 s (annealing and extension). The data were analyzed using Stratagene Mx 3000P software (Agilent Technologies), and the

expression levels of the target genes were normalized to the expression level of *GAPDH*.

Microarray Analysis. For microarray analysis, RNA samples were analyzed to assess concentration and integrity using the Agilent 2100 Bioanalyzer (Agilent Technologies) and amplified using the Illumina TotalPrep RNA amplification kit (Ambion) according to the manufacturer's instructions. Briefly, 500 ng of total RNA were reverse transcribed using the reverse transcriptase ArrayScript and converted into double-stranded DNA template for transcription of biotin-labeled cRNA. Concentration and quality of the purified labeled cRNA was assessed using the Agilent 2100 Bioanalyzer (Agilent Technologies) and 1.5 μg of total cRNA used for hybridization with the Illumina HumanHT-12 v4 Expression BeadChip Kit according to the manufacturer's recommendations. Expression data were processed with Illumina GenomeStudio software, using quantile normalization and background subtraction. Hierarchical cluster analysis was performed in GenomeStudio using the average signals of all lines and conditions investigated. To observe the molecular changes occurring upon osteogenesis of progenitor cells, average signals were log2-transformed and scatter plots generated using FlexArray 1.6.1 software (McGill University, Montreal, Canada). To account for the negative values generated after background subtraction, all values per condition were corrected adding a value of $|x| + 1$, where x corresponded to the most negative value generated for that condition. The percentage of genes with a fold change (FC) ≥ 3 between pairs of samples was calculated for all three cell lines investigated, and genes displaying a FC ≥ 3 further analyzed to identify common up- and down-regulated genes. Genes were further selected only if the gene was detected in at least one of the two conditions by the Illumina algorithm. To investigate possible interaction among proteins encoded by genes down-regulated and up-regulated in all three lines (defined by having a FC ≥ 3) following culture in bioreactors, the search tool STRING (http://string-db.org) was used to mine for recurring instances of neighboring genes. To increase the result validity, the analysis was restricted to include only experimentally determined protein interactions and database annotations. Functional classification of genes involved in osteogenesis per pairwise comparison was conducted using the Gene Ontology Annotation database (www.ebi.ac.uk/goa), with the genes displaying a FC ≥ 2 selected for further analysis.

In Vivo Implantation of Bone Constructs Cultured in Perfusion. Safety and stability of engineered bone constructs was assessed over 12 wk of s.c. implantation in immunodeficient mice (SCID-beige female mice; Harlan) according to the Columbia University Institutional Animal Care and Use Committee's approved animal protocol (AAAD8809). Animals were allowed to acclimate before the surgery and were anesthetized by isoflurane inhalation prior to construct implantation. Following a small incision along the vertebral axis of each animal, cultured bone constructs were implanted (one construct per mouse) into dorsal s.c. pockets. At the end of the experimental period, mice were anesthetized by inhalation of isoflurane and killed via cervical dislocation. Samples were harvested, washed in DPBS, and fixed 2 d in 10% (vol/vol) formalin in PBS before μCT imaging and histological analyses.

Histological Analyses. Cell/scaffold constructs before transfer to bioreactors, after perfusion culture (3 and 5 wk), and following 12-wk s.c. implantation in mice were washed in PBS, cut in half, and fixed in 10% (vol/vol) formalin at room temperature for 2 d. One-half of each construct was processed for histological and immunohistochemical analysis by decalcifying for 2 d with Immunocal solution (Decal Chemical Corp.), dehydration in graded ethanol solutions, paraffin embedding, sectioning to 5 μm, and mounting on glass slides. Samples were stained using routine H&E and Masson trichrome procedures.

For evaluation of bone matrix deposition and bone tissue vascularization, immunohistochemical staining was done using primary antibodies (all purchased from Millipore) against osteopontin (rabbit polyclonal anti-osteopontin; AB1870), bone sialoprotein (rabbit polyclonal anti-BSP II; AB1854), and osteocalcin (rabbit polyclonal anti-osteocalcin; AB10911). Human origin of engineered bone constructs following in vivo implantation was verified using primary antibodies against human nuclei (mouse monoclonal anti-human nuclei; MAB1281). Bone tissue vascularization in vivo was verified using primary antibodies against alpha smooth muscle actin (mouse monoclonal anti–α-SMA; 18-0160; Life Technology). Tissue sections were deparaffinized with CitriSolv, and rehydrated with a graded series of ethanol washes. The antigens were retrieved by incubation in citrate buffer (pH 6) at 90 °C for 30 min, and endogenous peroxidase activity blocked with H_2O_2 [3% (vol/vol)]. The sections were then blocked with serum and stained with primary antibodies overnight in a humidified environment, followed by the secondary antibody incubation, development with a biotin/avidin system, and counterstaining with Mayer's hematoxylin solution. The serum, secondary antibody, and developing reagents were obtained from Vector Laboratories Universal Vector Elite ABC Kit (PK6200). Negative controls were performed following the same procedure but omitting the primary antibody incubation.

Results of histological and immunohistochemical staining were documented by light microscopy under the same illumination, capture time, and white balance settings for all culture groups and negative staining controls with an Olympus IX71 using the Olympus DP2-BSW software. Collected images of H&E, Masson trichrome, and immunohistochemical stains were processed in Adobe Photoshop: image levels were adjusted from 0 to 255 to 50–200 to enhance the contrast for viewing; manually overlaid images were merged, cropped to optimal canvas size for all groups, and combined into figure panels using Adobe Illustrator.

Microcomputed Tomography. The μCT imaging was performed using a modification of a previously used protocol (5) with the following settings: voltage 55 kV, current 0.109 mA, slice thickness 21 μm, and interslice spacing 21 μm. Samples were scanned before seeding, after perfusion culture, and following 12-wk implantation in mice. Samples were aligned and stabilized along their axial direction inside microcentrifuge tubes, which were placed in the specimen holder of a vivaCT 40 system (SCANCO Medical AG). Samples were scanned at 21-μm isotropic resolution. The bone volume was obtained using a global thresholding technique with threshold at 220. Bone volume fraction, trabecular number, trabecular thickness, and trabecular spacing were determined with the structural reconstruction.

1. Boulting GL, et al. (2011) A functionally characterized test set of human induced pluripotent stem cells. *Nat Biotechnol* 29(3):279–286.
2. Hua H, et al. (2013) iPS derived beta cells model diabetes due to glucokinase deficiency. *J Clin Invest* 10.1172/JCI67638.
3. Chou BK, et al. (2011) Efficient human iPS cell derivation by a non-integrating plasmid from blood cells with unique epigenetic and gene expression signatures. *Cell Res* 21(3):518–529.
4. Marolt D, et al. (2012) Engineering bone tissue from human embryonic stem cells. *Proc Natl Acad Sci USA* 109(22):8705–8709.
5. Grayson WL, et al. (2011) Optimizing the medium perfusion rate in bone tissue engineering bioreactors. *Biotechnol Bioeng* 108(5):1159–1170.
6. Thomson JA, et al. (1998) Embryonic stem cell lines derived from human blastocysts. *Science* 282(5391):1145–1147.

A

LINE	TYPE	SEX	AGE	PASSAGE	SOURCE	DERIVATION METHOD	REPROGRAMMING FACTORS	REFERENCE
H9	hESC	F	N/A	34	Embryonic	IVF	-	**6**
H13	hESC	M	N/A	27	Embryonic	IVF	-	**6**
11C	hiPSC	M	36	63	Dermal fibroblasts	Retrovirus	OCT4-SOX2-KLF4	**1**
1013A	hiPSC	M	36	13	Dermal fibroblasts	Sendai virus	OCT4-SOX2-KLF4 c-MYC	**2**
BC1	hiPSC	M	31	48	Bone marrow	Episomal vector	OCT4-SOX2-KLF4 c-MYC-LIN28	**3**

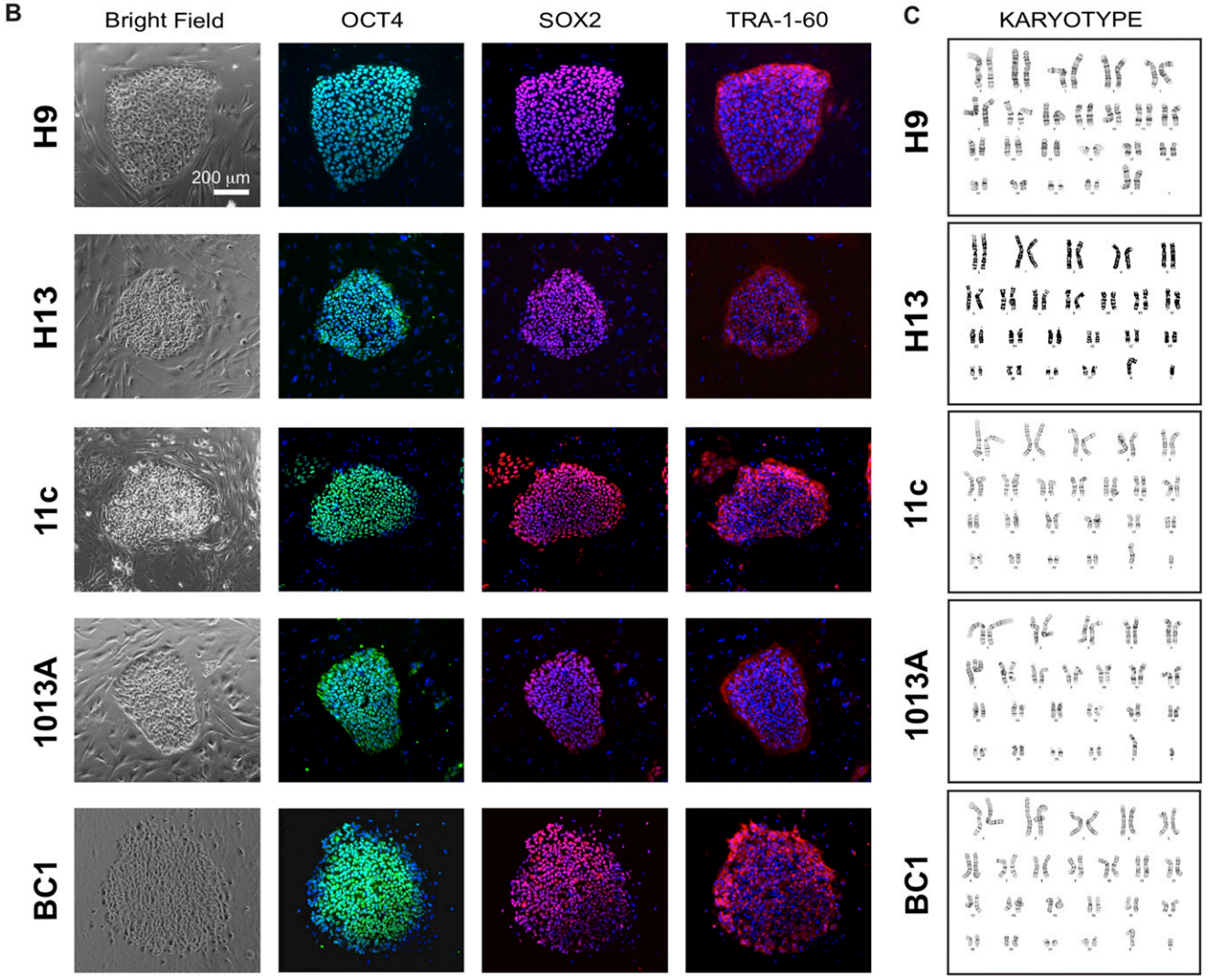

Fig. S1. The hESC and hiPSC lines used in this study. (*A*) Detailed information about cell origin and methods used to derive the pluripotent cell lines used in the study. (*B*) Immunofluorescence and (*C*) cytogenetic analyses of hESC lines H9 and H13, and hiPSC lines 11c, 1013A, and BC1. Upon expansion and before mesodermal induction, all cell lines expressed pluripotency markers OCT4 (green), SOX2, and TRA-1-60 (purple; nuclei, blue), and displayed a normal karyotype.

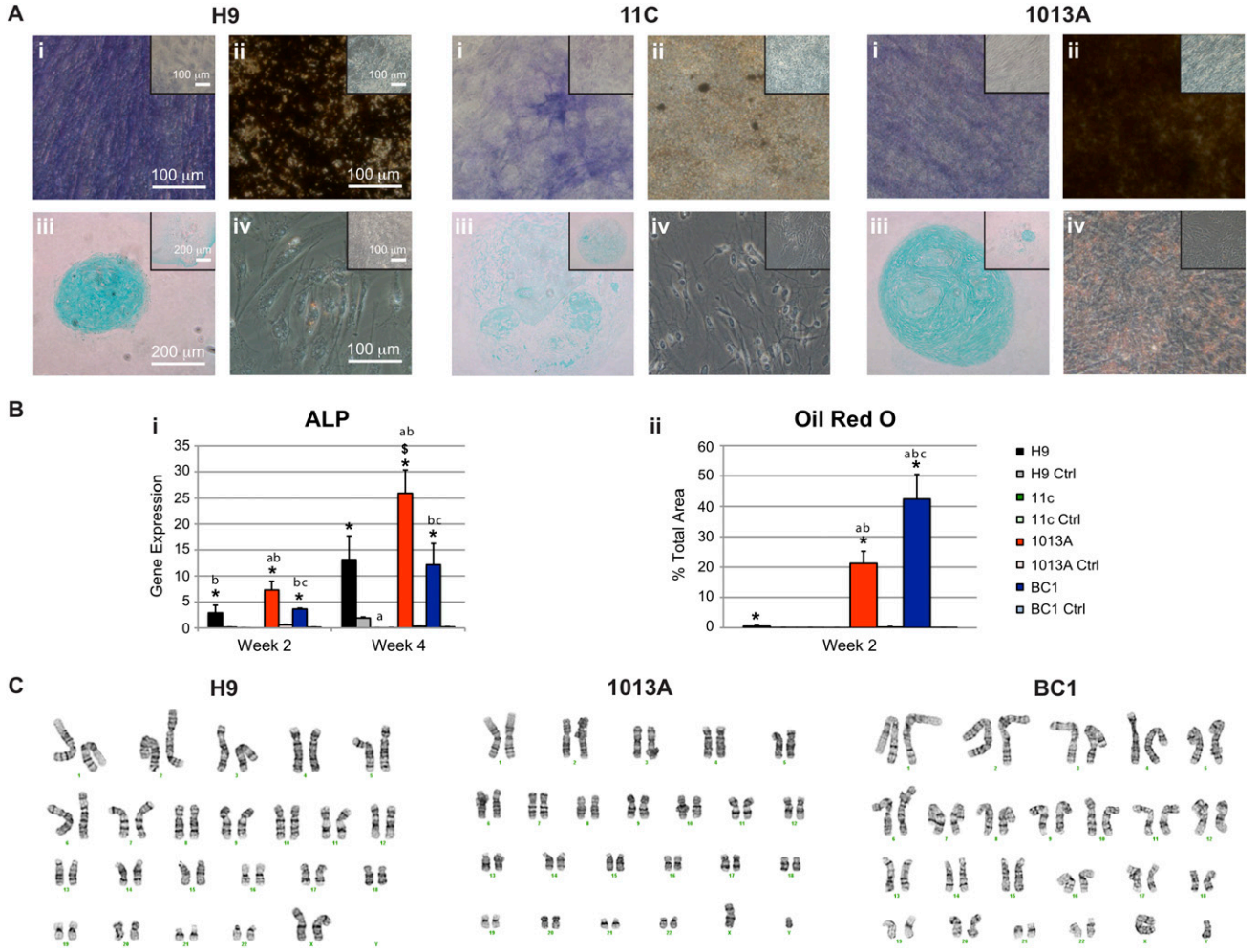

Fig. S2. In vitro differentiation potential and karyotype of mesenchymal progenitors. (*A*) Differentiation potential of H9-, 11c-, and 1013A-derived progenitors toward the osteogenic (*i*, *ii*), chondrogenic (*iii*), and adipogenic lineages (*iv*). (*A*, *i*) ALP staining (purple); (*A*, *ii*) von Kossa staining of deposited calcium (black); (*A*, *iii*) Alcian blue staining of GAG; (*A*, *iv*) Oil Red O staining of lipid vacuoles. (*Insets*) Cultures in control medium. (*B*) Expression of *ALP* after 2 and 4 wk in monolayer cultures (*i*); quantification of Oil Red O staining expressed as percent of stained area per total area (*ii*). Ctrl, control medium. Data represent averages ± SD ($P < 0.05$; asterisks denote significant difference between differentiation and control media at the same time point; $, significant difference between week 2 and week 4; a, difference to H9; b, difference to 11c; c, difference to 1013A). (*C*) Cytogenetic analysis of H9-, 1013A-, and BC1-derived progenitors following 10 passages in monolayer cultures, showing a normal karyotype for all cell lines investigated.

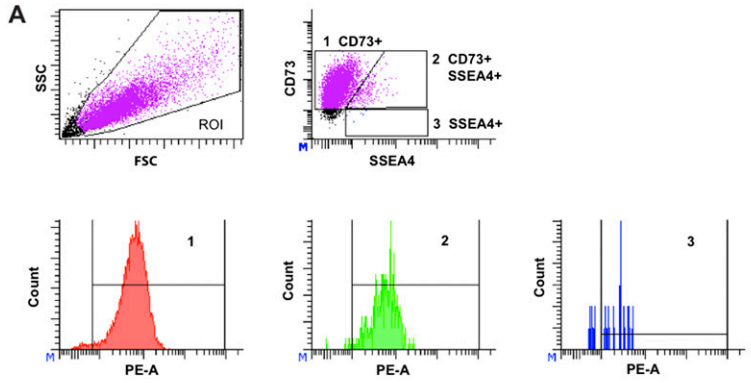

B

% Population expressing marker

<5 5-20 20-40 40-60 60-80 80-95 >95

Population	BMSC1			BMSC2			H9			1013A			BC1			11c		
Marker	% CD73+	% CD73+ SSEA4+	% SSEA4+	% CD73+	% CD73+ SSEA4+	% SSEA4+	% CD73+	% CD73+ SSEA4+	% SSEA4+	% CD73+	% CD73+ SSEA4+	% SSEA4+	% CD73+	% CD73+ SSEA4+	% SSEA4+	% CD73+	% CD73+ SSEA4+	% SSEA4+
HLA-A2	63.5	61.9	0.0	0.0	0.1	0.0	44.4	24.4	0.0	18.2	21.6	0.0	0.0	0.1	0.0	63.2	94.3	60.0
B2M	88.7	84.6	50.0	93.3	90.6	56.5	96.0	85.0	14.3	88.3	88.4	50.0	29.3	38.6	25.6	83.0	98.7	75.0
CD13	100.0	100.0	85.7	99.9	100.0	100.0	84.6	80.4	40.0	64.7	75.6	33.3	91.1	93.3	75.5	77.8	20.4	20.0
CD29	95.2	89.4	50.0	96.1	95.6	52.0	92.0	75.1	0.0	67.4	67.7	11.1	20.9	18.4	1.4	78.3	90.5	66.7
CD44	99.7	99.7	100.0	99.1	99.7	96.8	98.2	98.3	76.9	94.2	96.7	87.5	91.0	95.8	84.9	100.0	99.4	100.0
CD49e	96.2	95.0	80.0	93.6	97.9	61.1	98.7	94.0	44.4	89.9	92.0	16.7	90.5	90.0	80.4	91.2	64.8	33.3
CD90	99.3	98.4	100.0	99.4	99.1	95.7	87.6	83.3	58.3	99.1	99.2	100.0	98.9	99.5	94.8	98.5	88.8	100.0
CD151	99.5	98.6	33.3	99.7	99.4	78.4	98.9	95.7	45.5	98.1	98.3	56.3	97.1	97.9	90.3	99.8	99.3	70.0
ALP	78.7	70.6	87.5	32.8	20.8	33.3	7.4	7.2	0.0	8.0	11.5	0.0	8.4	9.2	3.4	3.1	5.0	9.1
CD49b	84.4	77.6	20.0	88.8	85.8	45.2	63.5	32.1	0.0	75.8	72.3	25.0	49.8	47.2	19.0	11.1	75.6	28.6
CD49c	44.0	26.6	33.3	51.1	45.7	15.2	83.2	52.3	0.0	65.6	67.6	22.2	36.8	31.5	10.3	36.3	74.9	60.0
CD49d	16.7	4.1	0.0	11.8	4.8	2.9	22.4	16.2	0.0	4.3	6.6	0.0	4.5	4.9	1.0	42.0	34.6	0.0
CD49f	30.6	22.3	0.0	23.9	34.3	0.0	39.4	19.6	0.0	46.2	55.0	12.5	38.9	38.2	14.3	22.0	40.2	0.0
CD51/61	10.1	6.7	0.0	5.5	3.1	0.0	31.3	18.1	0.0	0.6	0.3	0.0	4.5	2.0	1.1	3.9	5.0	0.0
CD54	44.3	29.9	14.3	35.0	20.6	0.0	61.2	45.9	33.3	54.3	53.3	27.3	10.6	11.5	5.2	14.5	13.9	9.1
CD81	74.9	60.7	60.0	66.2	57.8	11.4	80.3	51.4	0.0	62.1	63.3	16.7	30.0	31.9	14.8	63.6	49.5	42.9
CD140b	39.8	29.2	0.0	39.1	26.0	0.0	34.7	19.2	0.0	12.1	12.9	0.0	4.8	4.0	1.3	0.2	0.7	0.0
CD146	10.5	7.9	0.0	23.6	16.4	5.9	42.4	27.2	0.0	37.8	39.3	14.3	21.2	19.5	12.4	19.9	49.3	0.0
CD166	12.3	3.8	0.0	4.9	2.2	0.0	11.5	7.7	0.0	4.5	4.4	0.0	2.3	2.1	0.0	9.2	9.1	0.0
CD49a	14.6	11.4	0.0	11.8	5.5	0.0	7.0	9.2	0.0	0.2	0.1	0.0	0.3	0.0	0.0	8.4	39.7	6.7
CD63	10.6	4.6	16.7	5.4	4.0	0.0	12.9	5.0	0.0	1.9	1.4	0.0	0.5	0.3	2.1	13.8	3.3	0.0

Fig. S3. Flow cytometry characterization of surface antigen expression profiles of hiPSC and hESC-mesenchymal progenitor and BMSC subpopulations. (*A*) Gating strategy for analysis of CD73+, CD73+SSEA4+, and SSEA4+ subpopulations (*Upper*) expressing selected markers (labeled with phycoerythrin, PE) (*Lower*) in each cell line. (*B*) Expression patterns showing percentage of cells in the CD73+, CD73+SSEA4+, and SSEA4+ subpopulations expressing the marker, presented as heat maps (see color legend).

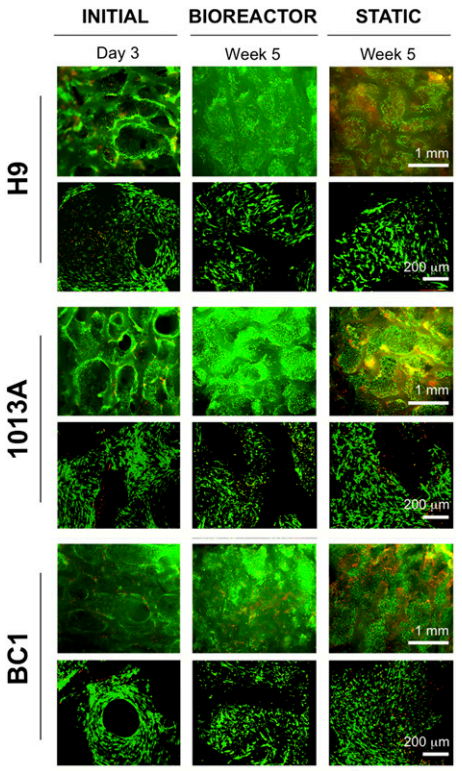

Fig. S4. Survival of H9-, 1013A-, and BC1-derived mesenchymal progenitors on decellularized scaffolds on day 3 after seeding, and week 5 of culture in perfusion bioreactors and static cultures. Live (green)/dead (red) staining of cell/scaffold constructs showed homogenous cell distribution. Cellularity and cell survival were higher in constructs cultured in perfusion bioreactors compared with static conditions. Epifluorescence micrographs (*Upper*); high-magnification confocal images (*Lower*).

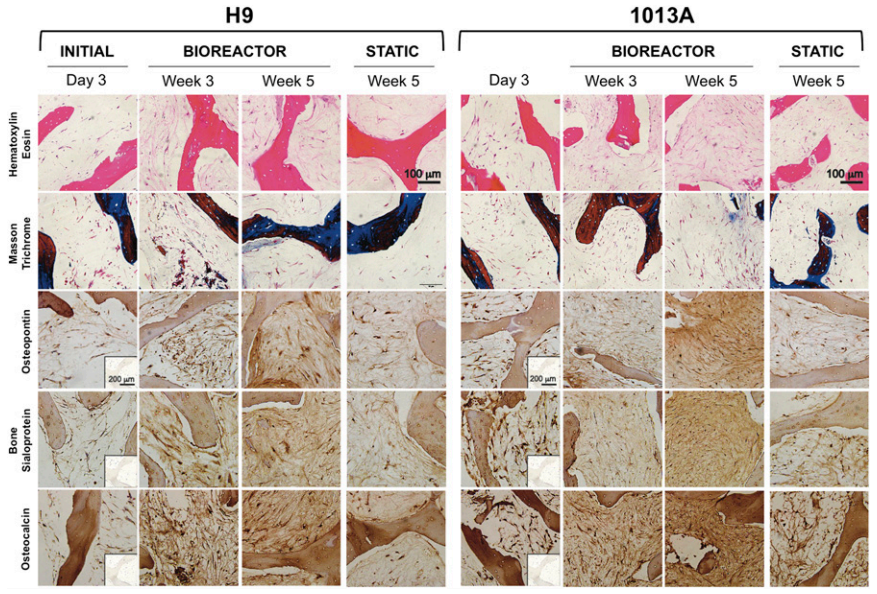

Fig. S5. Effects of bioreactor culture on bone tissue development. Histological analyses of seeded (day 3) and cultured (weeks 3, 5) constructs from H9- and 1013A-derived progenitors showed an increase in tissue formation over time, and denser tissue deposition in bioreactor compared with static group after 5 wk of culture (*Top*). Higher deposition of bone matrix proteins in perfusion bioreactor was confirmed by positive staining of collagen (Masson trichrome, blue; *Upper Middle*), osteopontin (brown; *Middle*), bone sialoprotein (brown; *Lower Middle*), and osteocalcin (brown; *Bottom*). Minimal staining was observed in constructs from static cultures. (*Insets*) Negative staining control.

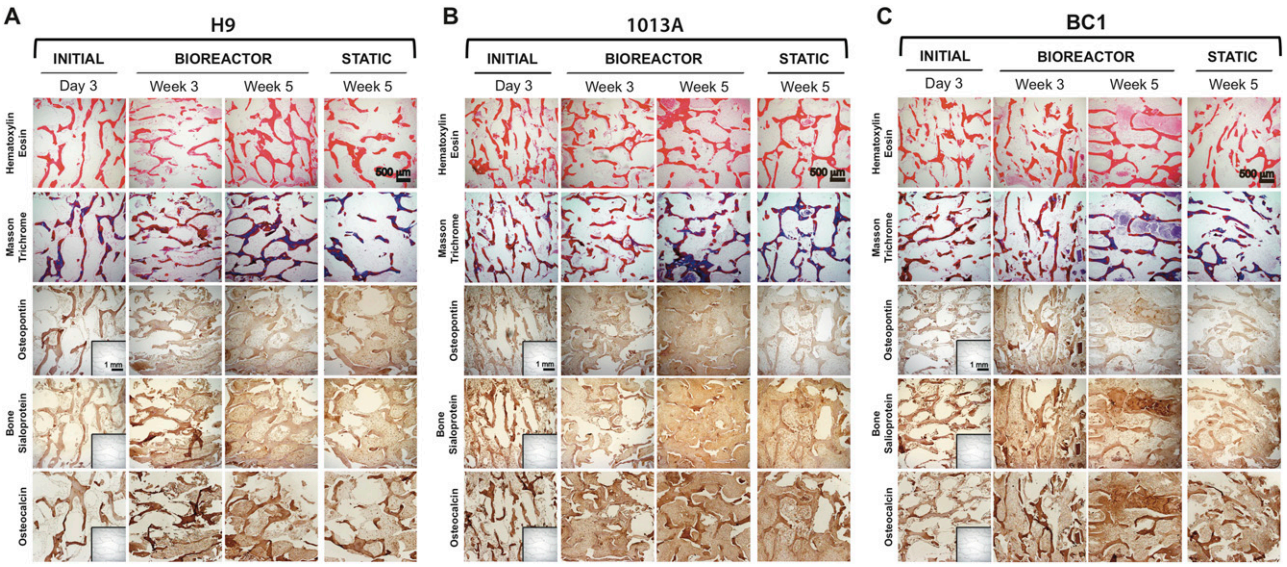

Fig. S6. Effects of bioreactor culture on bone tissue development. Low-magnification histological micrographs. Constructs of (*A*) H9-, (*B*) 1013A-, and (*C*) BC1-derived progenitors cultured for 5 wk in perfusion bioreactors showed uniform tissue formation and denser tissue matrix compared with constructs from static cultures (*Top*). Higher deposition of bone matrix proteins in perfusion bioreactor was confirmed by positive staining of collagen (Masson trichrome, blue; *Upper Middle*), osteopontin (brown; *Middle*), bone sialoprotein (brown; *Lower Middle*), and osteocalcin (brown; *Bottom*). Only minimal staining was observed in statically cultured constructs at weeks 3 and 5. (*Insets*) Negative staining control.

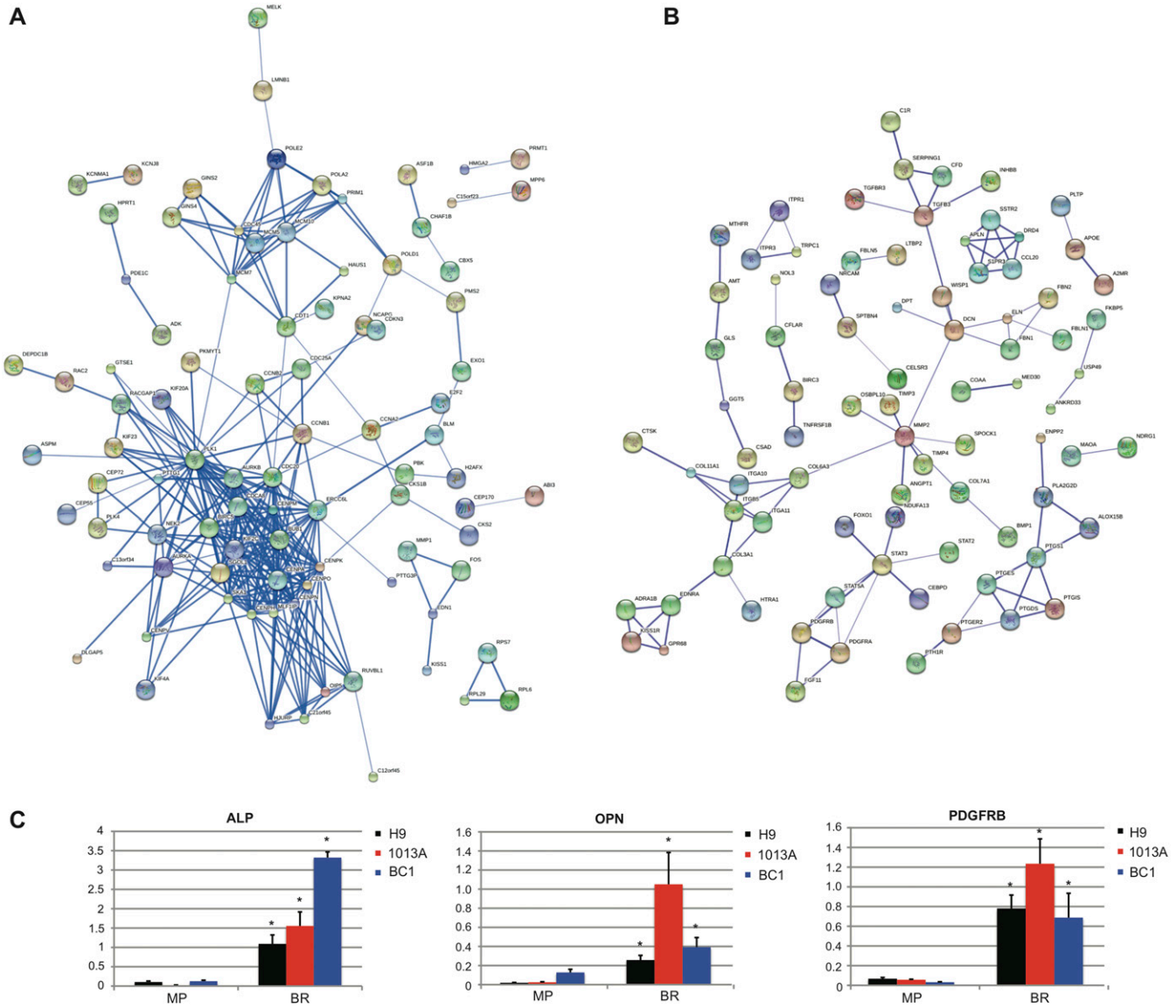

Fig. S7. Protein–protein interaction networks of genes differentially expressed in both hiPSC- and hESC-derived mesenchymal progenitors after bioreactor culture. (*A*) Genes commonly down-regulated in 1013A-, BC1-, and H9-derived progenitors following culture in bioreactors compared with mesenchymal progenitors prior to scaffold seeding. (*B*) Genes commonly up-regulated in 1013A-, BC1-, and H9-derived progenitors following culture in bioreactors compared with mesenchymal progenitors prior to scaffold seeding. Only connected nodes are shown. Proteins are identified as hubs if they have at least five protein interactions with the products of the connected genes. Stronger associations are represented by thicker lines. (*C*) Real-time PCR verification of microarray data showing strong activation of the bone-specific genes *ALP*, *OPN*, and *PDGFRB*. BR, bioreactor; MP, mesenchymal progenitor. Data represent averages ± SD (n = 3–4; $P < 0.05$; asterisk denotes significant difference between MP and BR).

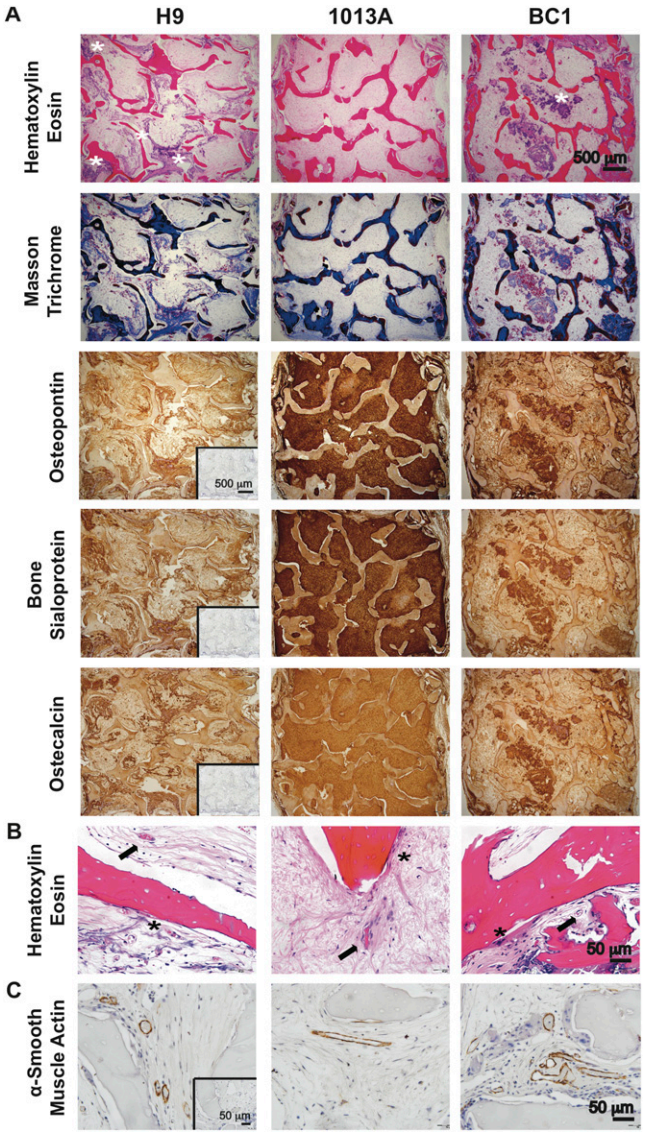

Fig. S8. Histological micrographs of engineered bone tissue after explantation. (*A*) Explanted samples were surrounded by loose connective tissue capsule. Stability of engineered bone and a uniform increase in tissue formation was documented by H&E staining (*Top*). High deposition of bone matrix proteins was confirmed by positive staining of collagen (Masson trichrome, blue; *Middle Upper*), osteopontin (brown; *Middle*), bone sialoprotein (brown; *Middle Lower*), and osteocalcin (brown; *Bottom*). (*Insets*) Negative staining control. Asterisks indicate regions of dystrophic ossification. (*B*) High-magnification micrographs of explanted bone. In all cases, signs of tissue vascularization (arrows mark microvessels) and remodeling (asterisks mark multinuclear osteoclastic cells overlaying the degrading scaffold surface) were observed. See also Fig. 5. (*C*) Alpha smooth muscle actin (α-SMA) staining (brown) confirming vascularization of engineered bone tissue for all lines investigated. (*Inset*) Negative staining control.

Table S1. Microarray expression data for a list of differentially expressed genes recognized to play a role during osteogenesis: H9 FC BR vs. MP

ILL_GENE	Definition	H9 FC BR vs. MP
ACVR1	Activin A receptor, type I	2.3
ALPL	Alkaline phosphatase, liver/bone/kidney	3.3
AXIN2	Axin 2 (conductin, axil)	2.9
BMP1	Bone morphogenetic protein 1	3.1
BMP6	Bone morphogenetic protein 6	2.3
CDH11	Cadherin 11, type 2, OB-cadherin (osteoblast)	2.5
COL11A1	Collagen, type XI, alpha 1, transcript variant B	14.5
COL12A1	Collagen, type XII, alpha 1, transcript variant long	31
COL15A1	Collagen, type XV, alpha 1	10.6
COL1A2	Collagen, type I, alpha 2	2
COL3A1	Collagen, type III, alpha 1	12.8
COL5A1	Collagen, type V, alpha 1	2.1
COL5A2	Collagen, type V, alpha 2	2.6
COMP	Cartilage oligomeric matrix protein	94.8
CTSK	Cathepsin K	48.4
EGR2	Early growth response 2 (Krox-20 homolog, *Drosophila*)	25.2
EIF2AK3	Eukaryotic translation initiation factor 2-alpha kinase 3	2.2
ENPP1	Ectonucleotide pyrophosphatase/phosphodiesterase 1	2.7
FGF2	Fibroblast growth factor 2 (basic)	2.3
FGFR1	Fibroblast growth factor receptor 1, transcript variant 4	2.1
FSTL3	Follistatin-like 3 (secreted glycoprotein)	2.8
IGF1R	Insulin-like growth factor 1 receptor	2.2
ITGA1	Integrin, alpha 1	4.4
KAZALD1	Kazal-type serine peptidase inhibitor domain 1	7.3
MGP	Matrix Gla protein	165.5
MMP14	Matrix metallopeptidase 14 (membrane-inserted)	2.3
MSX2	Msh homeobox 2	2.2
NAB1	NGFI-A binding protein 1 (EGR1 binding protein 1)	3.4
PDGFRB	Platelet-derived growth factor receptor, beta	3.8
PKDCC	Protein kinase domain containing, cytoplasmic homolog (mouse)	2.5
PTN	Pleiotrophin	2.8
SFRP1	Secreted frizzled-related protein 1	3.6
SLC26A2	Solute carrier family 26 (sulfate transporter), member 2	2.6
SORT1	Sortilin 1	4.4
STC1	Stanniocalcin 1	7.8
TGFB3	Transforming growth factor, beta 3	7.5
THRA	Thyroid hormone receptor alpha, transcript variant 2	2
TWIST1	Twist homolog 1 (*Drosophila*)	3.5
ADRB2	Adrenergic, beta-2-receptor, surface	−3.1
COL14A1	Collagen, type XIV, alpha 1	−2.5
CSF2	Colony stimulating factor 2 (granulocyte-macrophage)	−4.2
FN1	Fibronectin 1 (FN1), transcript variant 3	−3.1
ITGA3	Integrin, alpha 3	−3.2
MMP2	Matrix metallopeptidase 2	−9.4
MMP9	Matrix metallopeptidase 9	−44.9
MSX1	Msh homeobox 1	−2.4
PDGFA	Platelet-derived growth factor alpha polypeptide, transcript variant 2	−2.7
PDLIM7	PDZ and LIM domain 7, transcript variant 1	−3.9
PHEX	Phosphate regulating endopeptidase homolog	−2.6
PMF1	Polyamine-modulated factor 1	−3.1
PTHLH	Parathyroid hormone-like hormone, transcript variant 3	−4.6
SMAD1	SMAD family member 1, transcript variant 1	−3.7
SRGN	Serglycin	−2.3
TGFB2	Transforming growth factor, beta 2	−15.7
TUFT1	Tuftelin 1	−4.4
VCAM1	Vascular cell adhesion molecule 1, transcript variant 2	−3.4

List of genes up-regulated and down-regulated after 5 wk of bioreactor culture compared with initial in H9-derived progenitors. Genes expressing a fold change (FC) $\geq \pm 2$ are shown. Bold letters denote genes commonly up- or down-regulated in all analyzed lines. BR, bioreactor; MP, mesenchymal progenitor.

Table S2. Microarray expression data for a list of differentially expressed genes recognized to play a role during osteogenesis: 1013A FC BR vs. MP

ILL_GENE	Definition	1013A FC BR vs. MP
ALPL	Alkaline phosphatase, liver/bone/kidney, transcript variant 1	137.2
ATP6V1B1	ATPase, H+ transporting, lysosomal 56/58 kDa, V1 subunit B1	3.5
AXIN2	Axin 2 (conductin, axil)	3
BMP1	Bone morphogenetic protein 1, transcript variant BMP1-3	8.9
BMP3	Bone morphogenetic protein 3	2.6
BMP6	Bone morphogenetic protein 6	1.2
BMP8B	Bone morphogenetic protein 8b	2
CDH11	Cadherin 11, type 2, OB-cadherin (osteoblast)	4.1
COL10A1	Collagen, type X, alpha 1	8.7
COL11A1	Collagen, type XI, alpha 1, transcript variant B	51.6
COL12A1	Collagen, type XII, alpha 1, transcript variant long	11.6
COL15A1	Collagen, type XV, alpha 1	17.9
COL1A1	Collagen, type I, alpha 1	2.9
COL1A2	Collagen, type I, alpha 2	2.9
COL3A1	Collagen, type III, alpha 1	28.5
COL5A1	Collagen, type V, alpha 1	5.6
COL5A2	Collagen, type V, alpha 2	5
COMP	Cartilage oligomeric matrix protein	330
CTSK	Cathepsin K	69.4
ECM1	Extracellular matrix protein 1, transcript variant 1	2.1
EGR2	Early growth response 2 (Krox-20 homolog, *Drosophila*)	38.8
EIF2AK3	Eukaryotic translation initiation factor 2-alpha kinase 3	2
ENPP1	Ectonucleotide pyrophosphatase/phosphodiesterase 1	2.7
FSTL3	Follistatin-like 3 (secreted glycoprotein)	14.6
ICAM1	Intercellular adhesion molecule 1 (CD54)	10.3
IGF1R	Insulin-like growth factor 1 receptor	4.8
ITGA1	Integrin, alpha 1	13
KAZALD1	Kazal-type serine peptidase inhibitor domain 1	9.5
MEF2C	Myocyte enhancer factor 2C	2.3
MGP	Matrix Gla protein	137.5
MMP10	Matrix metallopeptidase 10 (stromelysin 2)	80.8
MMP14	Matrix metallopeptidase 14 (membrane-inserted)	4.1
MMP2	Matrix metallopeptidase 2	14.6
MMP9	Matrix metallopeptidase 9	2.5
MSX2	Msh homeobox 2	2.3
NAB1	NGFI-A binding protein 1 (EGR1 binding protein 1)	2
NAB2	NGFI-A binding protein 2 (EGR1 binding protein 2)	2.2
PDGFRB	Platelet-derived growth factor receptor, beta	12.3
SCARB1	Scavenger receptor class B, member 1	2
SLC26A2	Solute carrier family 26 (sulfate transporter), member 2	2.7
SORT1	Sortilin 1	6.5
SPP1	Secreted phosphoprotein 1, transcript variant 2	7.8
SUMF1	Sulfatase modifying factor 1	2.2
TFIP11	Tuftelin interacting protein 11, transcript variant 2	2.2
TGFB3	Transforming growth factor, beta 3	3.1
TGFBR1	Transforming growth factor, beta receptor 1, transcript variant 1	3.1
THRA	Thyroid hormone receptor alpha, transcript variant 2	7
TOB2	Transducer of ERBB2	2.1
VCAM1	Vascular cell adhesion molecule 1, transcript variant 2	2.8
VEGFA	Vascular endothelial growth factor A, transcript variant 3	2.8
VEGFB	Vascular endothelial growth factor B	2.1
ADRB2	Adrenergic, beta-2-, receptor, surface	−4.8
DEK	DEK oncogene (DNA binding)	−2.1
EXT1	Exostoses (multiple) 1	2
FGF1	Fibroblast growth factor 1 (acidic), transcript variant 1	−2.1
ITGA2	Integrin, alpha 2 (CD49B, alpha 2 subunit of VLA-2 receptor)	−2.5
MSX1	Msh homeobox 1	−2.8
NR1D1	Nuclear receptor subfamily 1, group D, member 1	−5.2
OSTF1	Osteoclast stimulating factor 1	−3
PTHLH	Parathyroid hormone-like hormone, transcript variant 3	−4.4
SMAD1	SMAD family member 1, transcript variant 1	−2.2

Table S2. Cont.

ILL_GENE	Definition	1013A FC BR vs. MP
SRGN	Serglycin	11
TGFB2	Transforming growth factor, beta 2	−98.2
TUFT1	Tuftelin 1	−2.8

List of genes up-regulated and down-regulated after 5 wk of bioreactor culture compared with initial in 1013A-derived progenitors. Genes expressing a fold change (FC) $\geq \pm 2$ are shown. Bold letters denote genes commonly up- or down-regulated in all analyzed lines.

Table S3. Microarray expression data for a list of differentially expressed genes recognized to play a role during osteogenesis: BC1 FCBR vs. MP

ILL_GENE	Definition	BC1 FCBR vs. MP
ALPL	Alkaline phosphatase, liver/bone/kidney	17.1
ATP6V1B1	ATPase, H+ transporting, lysosomal, V1 subunit B1	4.4
AXIN2	Axin 2 (conductin, axil)	2.3
BGN	Biglycan	2.2
BMP1	Bone morphogenetic protein 1, transcript variant BMP1-3,	4.5
BMP2	Bone morphogenetic protein 2	5.1
BMP3	Bone morphogenetic protein 3	2.4
CDH11	Cadherin 11, type 2, OB-cadherin (osteoblast)	4.2
COL10A1	Collagen, type X, alpha 1	66.6
COL11A1	Collagen, type XI, alpha 1, transcript variant B	11.8
COL12A1	Collagen, type XII, alpha 1, transcript variant long	14.1
COL14A1	Collagen, type XIV, alpha 1.	3.1
COL15A1	Collagen, type XV, alpha 1	65
COL1A1	Collagen, type I, alpha 1	4.1
COL1A2	Collagen, type I, alpha 2	5
COL3A1	Collagen, type III, alpha 1	28.2
COL5A1	Collagen, type V, alpha 1	4.4
COMP	Cartilage oligomeric matrix protein	1050.7
CTSK	Cathepsin K	48
DLX5	Distal-less homeobox 5	16.9
EGR2	Early growth response 2	730
FGF18	Fibroblast growth factor 18	2.5
FGF2	Fibroblast growth factor 2	3.3
FGFR1	Fibroblast growth factor receptor 1, transcript variant 4	7.5
FN1	Fibronectin 1, transcript variant 3	2.7
IBSP	Integrin-binding sialoprotein	2.4
ICAM1	Intercellular adhesion molecule 1	10.8
ITGA1	Integrin, alpha 1	32.1
KAZALD1	Kazal-type serine peptidase inhibitor domain 1	22.3
MGP	Matrix Gla protein	758
MMP10	Matrix metallopeptidase 10 (stromelysin 2)	161
MMP14	Matrix metallopeptidase 14 (membrane-inserted)	2.3
MMP2	Matrix metallopeptidase 2	5.3
PDGFRB	Platelet-derived growth factor receptor, beta	12.8
SFRP1	Secreted frizzled-related protein 1	2.7
TGFB1	Transforming growth factor, beta 1	4.7
TGFB3	Transforming growth factor, beta 3	8.7
THRA	Thyroid hormone receptor alpha, transcript variant 2	13.3
TWIST1	Twist homolog 1	2
VCAM1	Vascular cell adhesion molecule 1	129.7
VEGFA	Vascular endothelial growth factor A, transcript variant 3	5.2
VEGFB	Vascular endothelial growth factor B	2.5
ADRB2	Adrenergic, beta-2-, receptor, surface	−16.1
ENPP1	Ectonucleotide pyrophosphatase/phosphodiesterase 1	−2.2
EXT1	Exostoses (multiple) 1	−2.1
FGF1	Fibroblast growth factor 1 (acidic), transcript variant 1	−3.1
HTN3	Histatin 3	−16.4
MSX1	Msh homeobox 1	−2.6
PTHLH	Parathyroid hormone-like hormone, transcript variant 3	−2.3
SOX9	SRY (sex determining region Y)-box 9	−5.6
TUFT1	Tuftelin 1	−2.8

List of genes up-regulated and down-regulated after 5 wk of bioreactor culture compared with initial in BC1-derived progenitors. Genes expressing a fold change (FC) $\geq \pm 2$ are shown. Bold letters denote genes commonly up- or down-regulated in all analyzed lines.